

Dissolution at porous interfaces II *. A study of pore effects through rotating disc experiments

H. Grijseels **, L. van Bloois, D.J.A. Crommelin and C.J. de Blaey ***

Department of Pharmaceutics, Subfaculty of Pharmacy, University of Utrecht, Catharijnesingel 60, 3511 GH Utrecht (The Netherlands)

(Received July 30th, 1982)

(Accepted October 13th, 1982)

Summary

The intrinsic dissolution rate of 4 substances with different solubility (borax, nicotinic acid, disodium oxalate and theophylline) was measured by means of a rotating disc technique. Compressed pellets, mounted in a holder, were rotated in the dissolution medium at various speeds. The obtained results allow the calculation of the effective diffusion coefficients of the substances under examination.

Pores drilled into the surface of the pellets (pore diameter 0.20–2.00 mm) caused an increase of the dissolution rate because of changing hydrodynamics. The diameter of a drilled pore must exceed a critical value to bring about this rise in dissolution rate. Apart from the diameter, the depth of the pore is an important factor determining to what extent the dissolution rate is increased. The influence of the pore depth decreases with an increasing depth : diameter ratio.

The critical pore diameter was found to be the same (about 0.2 mm) for all the substances investigated. This implies that its size depends only on the hydrodynamic conditions (that are affected by the geometric change of the solid/liquid interface), and not on the physicochemical properties of the dissolving solid. Therefore these results have a general applicability for all compounds dissolving under similar hydrodynamic conditions.

* For part I, see *Int. J. Pharm.*, 9 (1981) 337–347.

** Present address: Cedona Pharmaceuticals B.V., P.O. Box 850, 2003 RW Haarlem, The Netherlands.

*** To whom correspondence should be addressed.

Introduction

Previous studies with a centrifugal stirrer apparatus (Van der Graaff et al., 1979; Grijseels and de Blaey, 1981) revealed that pores drilled in a tablet surface increase the dissolution rate of the surface. These studies were performed to gain a better insight into the mechanisms involved in the dissolution of solids at irregular interfaces. However, because of the complex streaming pattern in the apparatus used, it was impossible to correlate the increase in dissolution rate induced by the pores with the hydrodynamics at the tablet surface.

Therefore we switched to a rotating pellet system. Since the rotating disc method offers an excellent means of understanding the hydrodynamics, based on theory as well as experimental studies, we expected this would allow us to link the observed pore-effects with the actual hydrodynamic conditions.

The present article deals with the question whether the rotating pellet technique is a suitable tool for practical and theoretical research into the dissolution of porous surfaces, and presents results of experiments with 4 different substances studying the effect of various pore parameters.

Theoretical aspects of the rotating disc technique

Equations for the steady-state mass transfer at the surface of a rotating disc were mathematically solved by Levich (1962) for both the laminar and the turbulent diffusion regimen. His theoretical derivations have been proved to be valid in a large number of experimental studies. Most of the fundamental research with respect to the mass transfer at a rotating disc surface was performed in electrochemical experiments where the disc surface, or a part of it, acts as the electrode at which a reaction of a redox couple takes place. By measuring the limiting current passing through the disc electrode a value for the mass transfer rate is obtained.

Another application of the rotating disc, based on the same principles, is encountered in dissolution studies (Nogami et al., 1966, 1969; Prakongpan et al., 1976; Wu et al., 1976; Virtsava et al., 1978; Touitou and Donbrow, 1981). The mass flux or dissolution rate is determined by measuring the increase of the bulk concentration.

Both applications of the rotating disc system are completely comparable provided that the mass transport from or to the reacting surface is the slowest step in the overall mass transfer process. The rate of mass transfer finds its limitation in the diffusion layer established in the vicinity of the surface. The thickness of this layer, δ , is determined by the thickness of the hydrodynamic boundary layer (for a review, see Grijseels et al., 1981). Under laminar flow conditions the following relationship holds (symbols are listed at the end of the article):

$$\delta = 0.5 \cdot \left(\frac{D}{\nu} \right)^{1/3} \cdot d_n \quad (1)$$

where d_n , the thickness of the laminar boundary layer, is defined as

$$d_n = 3.6 \cdot \left(\frac{\nu}{\omega} \right)^{1/2} \quad (2)$$

From these equations it is clear that neither d_h nor δ depend on the radial position on the disc surface. Actually, this uniform accessibility is one of the great advantages of the rotating disc system. However, it must be stressed that the independence on the radial coordinate holds only for Reynolds numbers above about 100 (Millsaps and Pohlhausen, 1952; Riddiford, 1966). Below this Reynolds number smaller values for d_h occur with a minimum at $Re_c = 4$, noting that Re_c is defined as:

$$Re_c = \frac{x^2 \cdot \omega}{\nu} \quad (3)$$

A central zone always exists where d_h is smaller than on the remaining part of the disc surface. The radius of this central part amounts to about 3 mm at a disc rotating in water with a speed of 100 rpm, and increases with decreasing rotation velocities. This implies that the flux of dissolved material has a constant value from the entire pellet surface except for the central part where it is somewhat raised. The overall dissolution rate of the surface is a function of several parameters combined by Levich (1962) to one expression:

$$R = 1.9 \cdot \Delta C \cdot \nu^{-1/6} \cdot D^{2/3} \cdot r^2 \cdot \omega^{1/2} \quad (4)$$

This equation is limited to laminar hydrodynamic conditions which implies the absence of disturbing factors such as the occurrence of natural convection at very low rotation speeds or the rise of turbulence eddies at high revolution velocities. Eqn. 4 predicts a linear correlation between the dissolution rate, R , and the square-root of the angular velocity, ω , under laminar conditions. The proportionality factor in this relationship is composed of various physical parameters, viz. the effective diffusion coefficient, D , of the dissolving substance in the diffusion boundary layer, the concentration fall, ΔC , which under sink conditions is equivalent to the solubility of the solid, C_s , the kinematic viscosity of the solvent, ν , and the radius of the rotating surface, r . Most of these variables are easily obtainable from literature or experiment. In fact the only uncertain factor in Eqn. 4 is the magnitude of D . It is difficult to find for a specific combination of solute, solvent and temperature accurate values for D in the literature. Besides, as compared with D in an infinitely diluted solution, the effective diffusion coefficient during the dissolution process is decreased by the high solute concentration in the diffusion boundary layer. Rotating disc experiments furnish a simple method for the determination of effective diffusion coefficients of dissolving species by measuring the slope of the regression line obtained from dissolution rate data as a function of the square-root of the angular velocity.

Dissolution in presence of pores

Large pores in a pellet surface caused an increase of the dissolution rate (Wurster and Seitz, 1960). Van der Graaff et al. (1979) and Grijseels and de Blaey (1981) concluded from experiments that the size of such pores must exceed a critical value. Values were found for the minimal diameter of a drilled pore promoting the

dissolution rate to be in the range of 0.2–0.4 mm and depending on the hydrodynamic conditions. However, it must be stressed that the pore shape is not defined by its diameter alone. The depth of a drilled pore as well may influence to what extent the hydrodynamics near the dissolving surface, and thus the dissolution rate, are affected. Clearly a cylindrical pore is characterized completely by its depth and diameter, but as the pore shape is more asymmetric it becomes increasingly difficult to assign a meaningful size to the pore. In that case there is no one unique diameter or size for a pore and the same problems arise as in expressing size of non-spherical particles in terms of a meaningful diameter.

The promoting effect of a pore on the dissolution rate is the consequence of changed hydrodynamics near the dissolving surface. A turbulent flow pattern develops in the wake of a pore (Grijseels and de Blaey, 1981). The magnitude of the critical pore diameter is expected to be independent of the dissolving species. However, the increase of the dissolution rate due to pores larger than this critical size will be related to the solubility and the diffusion coefficient of the dissolving substance, since in a turbulent flow regimen R is proportional to the product $D^{3/4} \cdot C_s$ (Grijseels et al., 1981).

In the present paper we report on the results of experiments carried out to test this hypothesis.

Materials and methods

Test compounds

Four different substances were used for the dissolution rate experiments, viz. borax (disodium tetraborate decahydrate), nicotinic acid, theophylline monohydrate and disodium oxalate. They were primarily chosen on account of their range in solubility and their easy compressibility into tablets without the need of any additives. Borax, nicotinic acid and theophylline met the requirements of the European Pharmacopoeia (1969, 1971, 1975), disodium oxalate was of reagent grade (Merck, extra pure).

The solubilities in demineralized water at 20.0°C were obtained from the literature (theophylline) or determined experimentally (borax, disodium oxalate, nicotinic acid). A quantity of solute in excess of solution saturation was added to demineralized water. The resulting suspensions were mixed thoroughly and equilibrated at 20°C (48 h). After 24 and 48 h, samples were filtered and diluted to suitable concentrations for conductometrical analysis. In all cases equilibrium was reached within 24 h.

The procedure for manufacturing 15.0 mm-pellets of the pure substances and drilling pores into the pellet surfaces were described earlier (Grijseels and de Blaey, 1981). The diameter of the cylindrically shaped pores investigated in this study ranged from 0.20 to 2.00 mm. Their depth varied up to about 4 mm. The pores were drilled in such a geometric configuration that they formed a 'fairy ring' with a radius of 5.0 mm around the centre of the tablet surface. In the case of borax experiments the pores were filled with a saturated borax solution just before the dissolution test was run. During experiments with the other compounds it proved sufficient to use

demineralized water for this purpose because of the lower dissolution rates. Any remaining air bubbles were removed to ensure a complete wetting of the inner surface of the pores.

Dissolution assembly

The dissolution rate measurements were carried out in a rotating disc set-up shown in Fig. 1. The 1000 ml dissolution vessel, which was thermostatted at $20.0 \pm 0.2^\circ\text{C}$, met the requirements of USP XX (1980).

The tablets were mounted in a perspex holder, designed according to the recommendations given by Riddiford (1966) with respect to the shape of an optimally functioning rotating disc. Only one flat surface of the pellet was exposed to the dissolution medium. The shaft of the pellet holder was attached to an electronically controlled stirring motor permitting precision speed control (within 0.5%).

Dissolution procedure

About 550 ml of demineralized water was placed in the dissolution vessel and permitted to equilibrate to 20.0°C , whereby mixing was provided by means of a magnetic stirrer. Then, according to the pre-addition method described earlier (Grijseels and de Blaey, 1981), 10.0 ml of a solution containing a known quantity of the substance under study, was added to the content of the beaker. After sufficient mixing to obtain a homogeneous solution, the concentration was measured. This procedure provided an internal calibration during each dissolution test. Next, the magnetic stirrer was switched off and the already rotating pellet holder, in which a

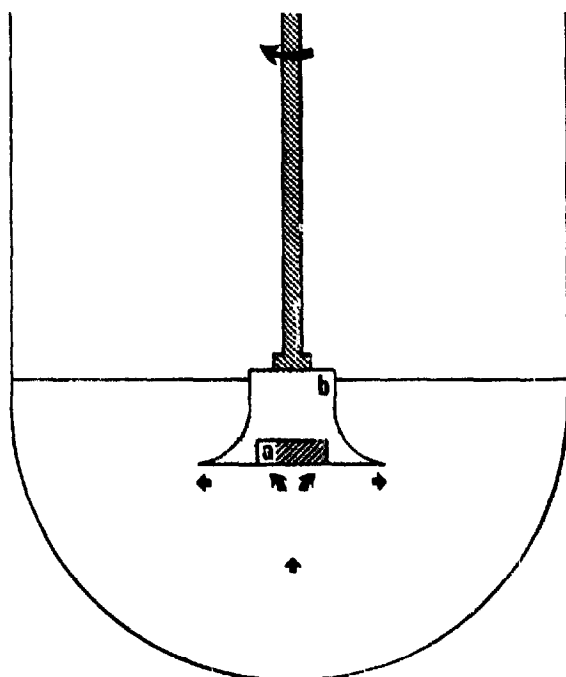


Fig. 1. Rotating pellet dissolution rate apparatus. (a) pellet; (b) holder.

tablet was mounted, was immersed in the dissolution medium. At this moment the actual dissolution experiment began. The duration of each dissolution test depended on the rotation speed of the pellet, to the effect that about the same quantity of the solid under examination had to dissolve at each rotation velocity. For this reason the experiments lasted between 140 and 480 s. Every run was performed at least in triplicate to allow for further statistical computations.

Analytical method

The concentration of the dissolved material in the solvent was recorded continuously during the experiments. Borax, disodium oxalate and nicotinic acid were assayed conductometrically by means of a conductivity cell mounted in the vessel. The recorder output of the conductometer was connected with a microcomputer assembly that collected the output signal 50 times every 10 s and computed and stored the mean value. After the dissolution experiment was finished, the least-squares regression line through the obtained data points was calculated and the slope of that line gave the dissolution rate of the tablet surface. In addition, the standard error of the estimate of the collected data with regard to the regression line was computed. This value never exceeded 0.5% of the mean conductivity during an experiment, indicating that all dissolution curves could be regarded as linear. In the case of nicotinic acid, the microcomputer software had to be adjusted, because of the fact that, in contrast with borax and disodium oxalate, the calibration curve of nicotinic acid is non-linear. The conductivity in this case increases, namely as a square-root function of the concentration, due to the decreasing degree of dissociation with increasing concentration.

During the experiments with theophylline the solution was analyzed spectrophotometrically at a wavelength of 270 nm. To that end the solvent was circulated continuously through a spectrophotometer to measure the absorbance. The obtained data were collected and handled by the on-line microcomputer in exactly the same manner as the conductivity data in order to calculate the dissolution rate values.

By subtracting the dissolution rates of intact pellet surfaces from those of surfaces with pores, and dividing the difference by the number of pores per pellet a value for the increase of the dissolution rate due to one pore, ΔR , was obtained.

pH

During some experiments, simultaneously with the conductance or the absorbance, the pH of the solvent was recorded to check whether difficulties could arise as consequence of changing pH. It appeared that amounts of theophylline or disodium oxalate dissolving during the experiment had no significant influence on the pH of demineralized water. The pre-addition of borax solution established a pH buffered at about 9.2 during the entire period of a dissolution test. Only in the case of nicotinic acid was the pH not constant during the actual experiment. Nevertheless, the continuous decrease of the pH did not affect the dissolution rate, as was examined by comparing the computed slopes of several parts of the dissolution curve.

Results and discussion

Smooth pellet surface

To test whether our rotating disc set-up agreed with the theoretical predictions, we measured the dissolution rate of intact tablet surfaces as a function of the angular velocity. Fig. 2 demonstrates that for the 4 compounds investigated, the dissolution rate is proportional to the square-root of the angular velocity. Besides the intercepts with the ordinate do not differ significantly ($P = 0.95$) from zero. These observations agree fully with Eqn. 4 indicating that the experimental conditions guarantee a laminar flow pattern near the smooth disc surface. Moreover, it is clear that under the chosen circumstances not the surface reaction, in which individual molecules are loosened from the crystal lattice, is the rate limiting step in the dissolution process, but the transport of dissolved molecules through the diffusion boundary layer. Such a diffusion-controlled behaviour is quite common for dissolution of solids in liquids (Cartensen, 1972), although a limited number of substances (hydroxyapatite, cholesterol, benzoic acid) are reported to be surface-reaction controlled (Wu et al., 1976; Prakongpan et al., 1976; Touitou and Donbrow, 1981). In Table I the parameters used to compute the diffusion coefficients from the slopes of the least-squares regression lines in Fig. 2 by means of Eqn. 4 are listed. The magnitude of the calculated diffusion coefficients is of the same order as values reported for similar substances (Higuchi et al., 1958; Nogami et al., 1966, 1969).

Pores in the pellet surface

During the dissolution experiments with tablet surfaces into which pores had been drilled, downstream to each pore a trough developed, which extended along a spiral trajectory over the surface (Fig. 3). The overall width and depth of the trough

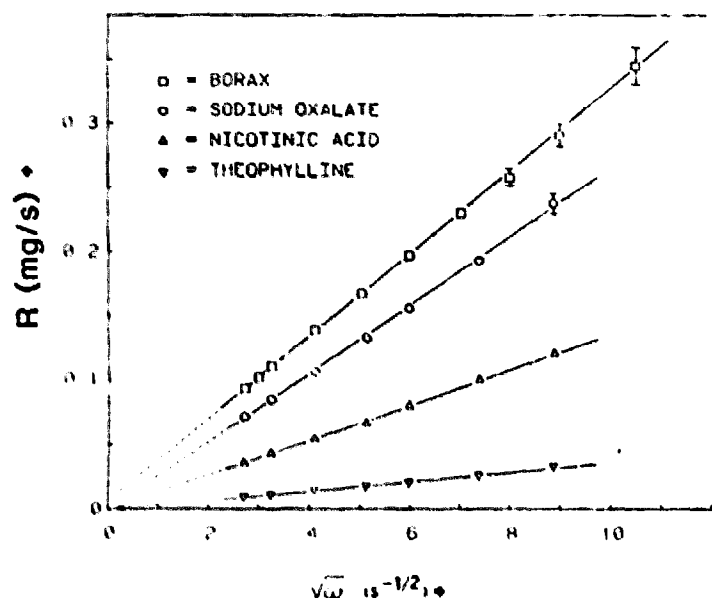


Fig. 2. Dissolution rate of smooth pellet surfaces versus the square-root of the angular velocity.

TABLE I
DIFFUSION COEFFICIENTS CALCULATED USING EQN. 4

	C_s ($\text{mg} \cdot \text{m}^{-3}$)	Slope ($\text{mg} \cdot \text{s}^{-1/2}$)	D ($\text{m}^2 \cdot \text{s}^{-1}$)
theophylline	5.10×10^6 ^a	3.75×10^{-3}	0.55×10^{-9}
nicotinic acid	15.4×10^6	13.53×10^{-3}	0.72×10^{-9}
disodium oxalate	33.2×10^6	26.54×10^{-3}	0.62×10^{-9}
borax	48.8×10^6	32.06×10^{-3}	0.47×10^{-9}

$r = 7.5 \times 10^{-3}$ m; $\nu_{\text{H}_2\text{O}}$ ^b = 1.004×10^{-6} $\text{m}^2 \cdot \text{s}^{-1}$; $\Delta C = C_s$ (sink conditions); $t = 20.0^\circ\text{C}$.

^a Fokkens et al (1983).

^b Handbook of Chem. and Phys. (1975).

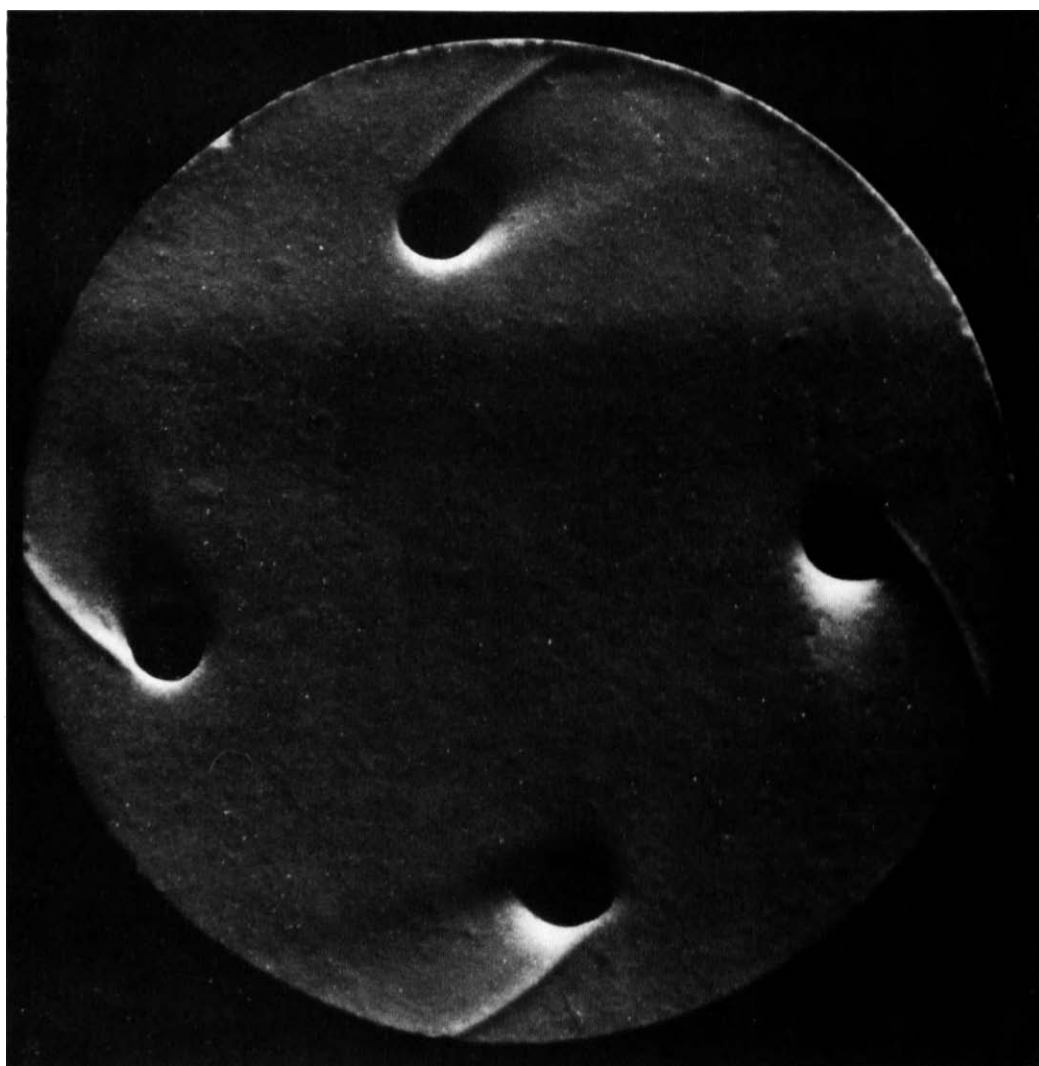


Fig. 3. Photograph of a tablet surface with drilled pores (pore diameter 1.00 mm) after the dissolution experiment.

increased with the pore diameter. Towards the edge of the tablet the channel broadened and shallowed. The side of the trough facing the tablet edge was bordered by a small ridge protruding above the tablet surface. Similar markings were observed at smooth surfaces by Riddiford (1966), Aimeur et al. (1973) and Virtsava et al. (1978). Riddiford attributed them to the onset of localized turbulence around a surface obstruction, causing an enhanced rate of mass transfer. Deslouis et al. (1977) mention that local roughnesses on an electrode surface can cause turbulence in the wake of the obstacle by lowering the critical Reynolds number. On the other hand, Rogers and Taylor (1963) report in a mainly qualitative study of the spirals developing behind small protrusions, that no indication of turbulence was found in any of the spirals examined. It must be emphasized that the protrusions they studied were very small as compared with the pore dimensions in our investigations. From the curvature of the spirals they deduced that the height of the protrusions was only about 10–20 μm . In the same study, autoradiographic experiments indicated a lower mass flux at the spirals than at the uniform surface, which should imply that an increased flux at the trough is predominated by the reduced mass transfer from the ridge.

In all dissolution experiments described hereafter, which were used for further calculations and interpretations, we adjusted the number of pores in such a manner that a visible overlap of the troughs in the tablet surface was avoided. By varying the number of pores per tablet we verified that the pores acted independently of each other.

Pore depth

Fig. 4 shows the results of dissolution experiments with borax tablets into which pores of varying diameter and depth were drilled. The increase of the dissolution rate per pore, ΔR , is plotted against the pore depth. It is clear from the initially higher slope of the lines that for every diameter ΔR of shallow pores is more sensitive to depth variation than ΔR of deep pores. Comparison of the 4 graphs leads to the conclusion that, regarding relatively deep pores, the influence of the depth decreases with decreasing pore diameter. For pores with a diameter below 1.5 mm and a depth : diameter ratio above about 1.5, the pore diameter is the dominant parameter with respect to the dissolution rate-increasing effect of such pores.

Pore diameter

To investigate the relationship between pore diameter and dissolution rate more extensively, we varied the pore diameter between 0.20 and 1.50 mm. In pursuance of the results obtained from the pore depth experiments, the pores were drilled with a depth that always exceeded their diameter by about 1 mm.

Fig. 5 shows the relationship between ΔR and the pore diameter of these pores characterized by a relatively large depth : diameter ratio. For the 4 substances investigated, a distinct linear correlation seems to exist between those two variables. From the least-squares regression lines through these data the critical pore diameters were computed (Table 2). These values prove that d_{crit} is independent of the physicochemical properties of the dissolving solid. This is important, since it implies

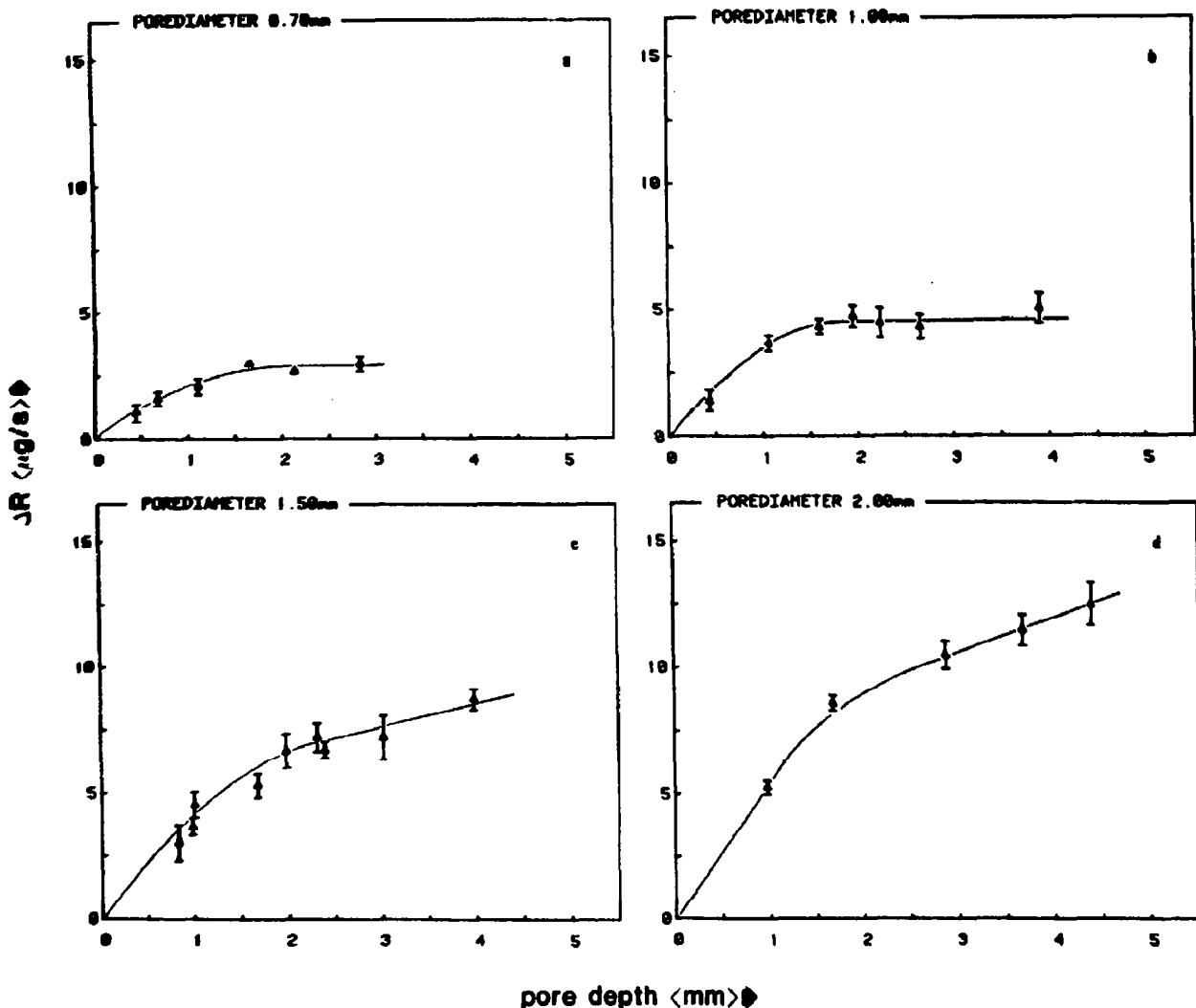


Fig. 4. Increase of the dissolution rate per pore (ΔR) as a function of the pore depth for different pore diameters. Rotation speed 100 rpm ($\omega^{1/2} = 3.24 \text{ s}^{-1/2}$). Dissolving substance: borax. (a) pore diameter 0.70 mm; (b) 1.00 mm; (c) 1.50 mm; (d) 2.00 mm. Vertical bars represent the standard deviations ($n \geq 3$). If not shown they fall within the drawn symbol.

TABLE 2

CRITICAL PORE DIAMETER DETERMINED AT A ROTATION VELOCITY OF 160 rpm ($\omega^{1/2} = 4.09 \text{ s}^{-1/2}$) WITH DIFFERENT DISSOLVING SUBSTANCES. THE VALUES AND STANDARD DEVIATIONS ARE CALCULATED FROM THE LEAST-SQUARES REGRESSION LINES IN FIG. 5.

	d_{crit} (mm)
theophylline	0.19 ± 0.01
nicotinic acid	0.20 ± 0.03
disodium oxalate	0.19 ± 0.04
borax	0.18 ± 0.03

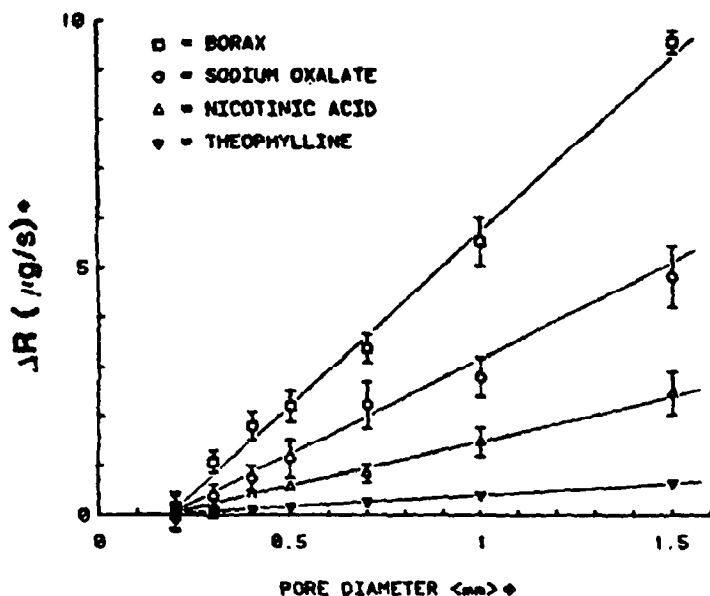


Fig. 5. Increase of the dissolution rate per pore (ΔR) as a function of the pore diameter. Rotation speed 160 rpm ($\omega^{1/2} = 4.09 \text{ s}^{-1/2}$). The data points are connected by the least-squares regression lines. Vertical bars represent the standard deviations. If not shown they fall within the drawn symbol.

that studies such as the present one into the role of pores at dissolving interfaces can be performed with a model substance. The experimental observations and results obtained with such a model substance can then be generalized for other solid/solvent systems where similar hydrodynamic conditions are present.

Fig. 6 is a log-log plot of the slopes of the regression lines in Fig. 5 versus the species dependent product $D^{3/4} \cdot C_s$. Since the increase of the dissolution rate due to

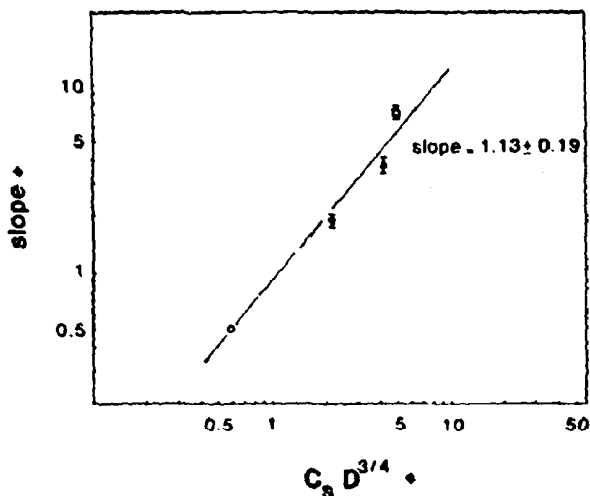


Fig. 6. The slopes of the lines in Fig. 5 ($\text{mg} \cdot \text{m}^{-1} \cdot \text{s}^{-1}$), representing the dependence of ΔR on the pore diameter, as a function of the species dependent product $D^{3/4} \cdot C_s$ ($\text{mg} \cdot \text{m}^{-3/2} \cdot \text{s}^{-3/4}$). \square , borax; Δ , disodium oxalate; ∇ , nicotinic acid; \circ , theophylline. Vertical bars represent the standard deviations.

a pore is believed to be the consequence of turbulence developed in the wake of that pore, a linear correlation between these two quantities is expected.

The calculated slope of the regression line of the logarithmic graph is 1.13 with a standard deviation of 0.19 and does not differ significantly from unity.

This is another indication that the influence of pores on the dissolution rate is purely caused by a change of the hydrodynamic conditions near the dissolving surface.

Abbreviations

C_s	solubility ($\text{mg} \cdot \text{m}^{-3}$)
D	diffusion coefficient ($\text{m}^2 \cdot \text{s}^{-1}$)
d_{crit}	critical pore diameter (mm)
d_n	thickness of the hydrodynamic boundary layer (mm)
P	probability
R	dissolution rate ($\text{mg} \cdot \text{s}^{-1}$)
r	radius of the pellet surface (mm)
Re_x	local Reynolds number
t	temperature ($^{\circ}\text{C}$)
x	radial distance from the centre of the disc surface (mm)
ΔC	concentration difference in the diffusion boundary layer ($\text{mg} \cdot \text{m}^{-3}$)
ΔR	increase of the dissolution rate due to one pore ($\text{mg} \cdot \text{s}^{-1}$)
δ	thickness of the diffusion boundary layer (mm)
ν	kinematic viscosity ($\text{m}^2 \cdot \text{s}^{-1}$)
ω	angular velocity (s^{-1})

References

- Aimeur, F., Daguinet, M., Kermiche, F. and Meklati, M., *Theorie et applications des microelectrodes*. *Electrochim. Acta* 18 (1973) 87–93.
- Carstensen, J.T., *Theory of Pharmaceutical Systems*, Vol. I, Academic Press, New York, 1972, pp. 219–241.
- Deslouis, C., Epelborn, I., Keddani, M., Viet, L., Dossenbach, O. and Ibl, I., *Recent progress in methodology of the rotating disk electrode*. In Spalding, D.B. (Ed.), *Physicochemical Hydrodynamics*, Advance Publications, London, 1977, Part 2, pp. 939–971.
- European Pharmacopoeia, 1969, Vol. I, pp. 263–265; 1971, Vol. II, pp. 384–385; 1975, vol. III, pp. 133–134.
- Fokkens, J.G., van Amelsfoort, J.G.M., de Blaey, C.J., de Kruif, C.G. and Wilting, J., *A thermodynamic study of the solubility of theophylline and its hydrate*. *Int. J. Pharm.* (1983) in press.
- Graaff, H. van der, de Boer, B.B. and de Blaey, C.J., *The role of pores in dissolution processes*. *Int. J. Pharm.* 3 (1979) 293–297.
- Grijseels, H., Crommelin, D.J.A. and de Blaey, C.J., *Hydrodynamic approach to dissolution rate*. *Pharm. Weekbl. Sci. Edn.* 3 (1981) 129–144.
- Grijseels, H. and de Blaey, C.J., *Dissolution at porous interfaces*. *Int. J. Pharm.* 9 (1981) 337–347.
- Handbook of Chemistry and Physics*, Weast, R.C. (Ed.), C.R.C. Press, Cleveland, OH, 1975, pp. F11 and F49.

- Higuchi, W.I., Parrott, E.L., Wurster, D.E. and Higuchi, T., Investigation of drug release from solids II. Theoretical and experimental study on influences of bases and buffers on rates of dissolution of acidic solids. *J. Am. Pharm. Ass. Sci. Edn.* 47 (1958) 376-383.
- Levich, V.G., *Physicochemical Hydrodynamics*, Prentice Hall, Englewood Cliffs, 1962, pp. 139-184.
- Millsaps, K. and Pohlhausen, K., Heat transfer by laminar flow from a rotating plate. *J. Aeron. Sci.* 19 (1952) 120-126.
- Nogami, H., Nagai, T. and Suzuki, A., Studies on powdered preparations XVII. Dissolution rate of sulfonamides by rotating disk method. *Chem. Pharm. Bull.*, 14 (1966) 329-338.
- Nogami, H., Nagai, T. and Yotsuyanagi, T., Dissolution phenomena of organic medicinals involving simultaneous phase changes. *Chem. Pharm. Bull.*, 17 (1969) 499-509.
- Prakongpan, S., Higuchi, W.I., Kwan, K.H. and Molokhia, A.M., Dissolution rate studies of cholesterol monohydrate in bile acid-lecithin solutions using the rotating disk method. *J. Pharm. Sci.*, 65 (1976) 685-689.
- Riddiford, A.C., The rotating disk system. In Delahay, P. (Ed.), *Advances in Electrochemistry and Electrochemical Engineering*, Vol. 4, Interscience, New York, 1966, pp. 47-116.
- Rogers, G.T. and Taylor, K.J., Effect of small protrusions on mass transport to a rotating disk electrode. *Nature (Lond.)*, 200 (1963) 1062-1064.
- Touitou, E. and Donbrow, M., Deviation of dissolution behaviour of benzoic acid from theoretical predictions with lowering of temperature: limitations as a model dissolution substance. *Int. J. Pharm.*, 9 (1981) 97-106.
- United States Pharmacopeia, 1980, 20th Rev., p. 959.
- Virtsava, L.A., Dzelme, Y.R., Tiliks, Y.E. and Bugaenko, L.T., Kinetics of dissolution of potassium chloride in water from a rotating disk. *Russ. J. Phys. Chem.*, 52 (1978) 1638-1641.
- Wu, M.S., Higuchi, W.I., Fox, J.L. and Friedman, M., Kinetics and mechanism of hydroxyapatite crystal dissolution in weak acid buffers using the rotating disk method. *J. Dent. Res.*, 55 (1976) 496-505.
- Wurster, D.E. and Seitz, J.A., Investigation of drug release from solids III. Effect of changing surface-weight ratio on the dissolution rate. *J. Am. Pharm. Ass. Sci. Edn.*, 49 (1960) 335-338.